EXARC JOURNAL 2026/3
18 Articles | Open Access

Reviewed Article:

Experimental Smelting of Local Copper Ores from Moravia

Persistent Identifier: https://exarc.net/ark:/88735/10862

EXARC Journal Issue 2026/3 | **Publication Date:** 2026-08-21

Author(s): Filip Ševčík [1] ✉, Matěj Kmošek [2], Čeněk Fouček [2]

[1] Department of Archaeology and Museology, Faculty of Arts, Masaryk University, Czech Republic

[2] Institute of Archaeology of the Czech Academy of Sciences, Brno, Czech Republic

This paper presents the results of experimental smelting of local copper ores from two sites in Moravia, Czech Republic (Štěpánov nad Svratkou and Lipová-lázně), aimed at testing whether these small, previously unstudied deposits were suitable for prehistoric copper production. High-purity malachite from the Shilu mine (China) served as a reference ore. A hemispherical, partially sunken furnace was used together with three ore-charging methods (graphite crucible, clay ball, direct furnace charge) and two air-supply systems (lever-operated

bellows and elder blowpipes). Both Moravian ores were successfully reduced to metallic copper of high purity (>99%), confirming their smeltability despite lower copper content and higher gangue proportions than the reference ore. Yields varied considerably between ores and charging methods. XRF analysis showed selective transfer of trace elements from ore to metal: silver became the dominant impurity in copper from Štěpánov nad Svratkou, while manganese, cobalt and nickel characterised copper from Lipová-lázně; arsenic transfer was consistently limited, suggesting that the elevated arsenic levels typical for example of Mondsee-type copper required deliberate addition of arsenic-rich ore rather than occurring naturally during smelting.

> The experiment aimed to answer one main research question and several sub-questions. The main research question was whether local copper ores from the Moravian region were of sufficient quality to be successfully reduced to pure copper. The other research sub-questions were whether this result could be achieved using technology roughly corresponding to the Eneolithic period.

Introduction

At present, we have a fairly good overview of the distribution networks of copper raw material in prehistory, at least regarding the main regions from which a significant portion of the utilised copper originated. Systematic research conducted by a number of scholars and research projects, employing a wide range of analytical methods, has gradually clarified key questions related to copper sources – from Eneolithic mining in the Balkans (Radivojević, *et al.,* 2021), through mining activities on the Iberian Peninsula (Hunt Ortiz, 2003), to the intensive exploitation of Alpine deposits in the Mitterberg region (Pernicka, Lutz and Stöllner, 2016).

From the prehistoric period, a total of 47 sites with confirmed copper mining activities are currently known (O'Brien, 2014, Figure 1.10). Many of these sites had considerable supra-regional significance at the time, with the east Alpine region supplying vast areas of Central Europe serving as a typical example (O'Brien, 2014, p. 163). In addition to these major centres, there is also evidence of sites of regional or local character, for example, on certain Greek islands, where mining activity in the third millennium BC is generally characterised as small-scale and spatially dispersed (O'Brien, 2014, p. 58). Another relevant example is Špania Dolina in Slovakia, where mining activity has been documented for the Eneolithic period (Točík and Žebrák, 1989).

In the Balkan region, several sites of supra-regional importance emerged during the Eneolithic period. One such example is Majdanpek, which has been associated with Mondsee-type copper. This copper circulated during the fourth millennium BC across large areas of Europe, particularly from the Balkans to Central Europe (Pernicka and Frank, 2015). Another important site is the Ai Bunar in Bulgaria, known for its extensive mining activity (Radivojević

and Roberts, 2021, p. 18). At the same time, sites of more regional character were present (Radivojević and Roberts, 2021, pp. 18–19).

Despite significant progress in research, the potential use of smaller, locally significant ore deposits in some areas remains an open question, including the present-day territory of the Czech Republic, with the occurrence of smaller copper deposits. It is assumed that even very limited local sources may have been exploited as early as the Eneolithic period, when they could have been relatively quickly and efficiently 'exhausted' by local prospectors (Zachar and Salaš, 2019, p. 622). However, this possibility is significantly limited by the smelting expertise of these potential prospectors, even with the presence of accessible and known deposits.

Research in the Czech Republic has so far focused primarily on deposits in the Krušné hory (Erzgebirge) area (Niederschlag, *et al.*, 2003; Zachar and Salaš, 2019). However, the occurrence of copper minerals elsewhere in the Czech territory is not uncommon (Burkart, 1953; Kruťa, 1966; 1973), which at least hypothetically allows for opportunistic use in prehistory. One such site is, for example, a partially investigated location in the cadastral area of Mutěnín, where copper ores with evidence of mining activities occur near a prehistoric settlement (Chmelíková, 2014; Kmošek, *et al.*, 2025). The key question, however, remains whether local copper ore sources achieved such qualitative and quantitative parameters that would allow their successful transformation into metallic copper using prehistoric technological methods. For this reason, in October 2023 and May 2024, a series of experimental smelts was conducted, aiming to test how smeltable the local copper ores from two sites in Moravia are.

The success of copper smelting depends not only on ore quality but also on the entire technological system, including fuel, furnace construction, air supply, and the behaviour of ceramic components under high temperatures. Experimental studies have shown that these factors can significantly influence both the course of the reduction process and the nature of the resulting byproducts, including slag and metallurgical debris (Rose, Fabian and Goren, 2021).

One of the key variables in prehistoric metallurgy is the method of air supply to the furnace. While blowpipes are often assumed to represent a simple and widespread solution, experimental studies suggest that this assumption may not always be justified. In some cases, alternative systems such as bellows may have offered greater efficiency and reduced physical demands on the operators. This issue remains particularly relevant when evaluating the feasibility of different smelting techniques.

Beyond testing the feasibility of metal production, experimental smelting provides valuable insights into the formation of metallurgical byproducts and their archaeological visibility. The structure and composition of slag, vitrification of ceramic materials, and the presence of copper prills can all be better understood through controlled experiments, thereby improving

the interpretation of archaeological assemblages. At the same time, it is important to emphasize that experimental results do not represent exact reconstructions of prehistoric practices but rather test the plausibility of specific technological scenarios. Variability in raw materials and experimental conditions means that such results should be interpreted as indicative rather than definitive (Rose, Fabian and Goren, 2021).

Material

For the purpose of the experiment, raw materials from three sites were used (two of them from Moravia; See Figure 1). In all cases, the minerals were secondary copper minerals, which occur in the upper, so-called oxidation zone of copper deposits, especially copper carbonates. These minerals form through the oxidation of primary copper minerals, primarily due to their proximity to the Earth's surface and the action of percolating water (O'Brien, 2014, pp. 2-8).

The first site from which copper ores originated is Štěpánov nad Svratkou, located in the Bohemian-Moravian Highlands, where the material was obtained through prospecting activities of the main author. The area around Štěpánov nad Svratkou represents an important polymetallic ore deposit, known as the Štěpánov mining district, where mining is documented from the 13th century until the 20th century (Pařízek, 2000, pp. 5–6). Many old mining activities have been preserved here, particularly in the vicinity of the settlement of Borovec, where intensive mining and prospecting activities took place (Houzar, *et al.*, 2000). Copper minerals found in the area include malachite, azurite, chalcopyrite, cuprite, bornite, bournonite, brochantite, covellite, chalcophyllite, chalcocite, chrysocolla, tetrahedrite, and native copper (Pařízek, 2000, p. 6). Most of the material used for the experiments comes from secondary accumulations in the forefield of the Mír adit. Among the collected minerals, malachite overwhelmingly predominates, with smaller amounts of azurite and chalcopyrite present (See Figures 2 and 3).

The second site is Lipová-lázně, located in the Hrubý Jeseník Mountains. In this case as well, the material was collected directly on site. In the surroundings of Lipová-lázně, there are several locations with sulfide mineralization associated with hydrothermal veins (See Figure 4), and some of these locations were even subject to small-scale mining attempts (Kruťa, 1973, p. 394; Dolníček, Nepejchal and Vrtiška, 2024, p. 8). An example is the Brloh site, with an adit and spoil heaps on the southern slope of Kopřivný Hill, where mining was focused on chalcopyrite mineralization (Kruťa, 1973, p. 131). For prospecting, a location was selected on the summit of Smrčník Hill, today a quarry for calcitic marble. The mineralization is associated with steep, nearly vertical veins in the marble, ranging in thickness from a few centimetres to over 1 m. The waste material contains quartz and various forms of calcite, while the main ore minerals are chalcopyrite and galena, with pyrite, sphalerite, silver, pyrolusite, and goethite occurring less frequently. Supergene minerals include limonite, stilpnosiderite, malachite, azurite, alophane, chrysocolla, cerussite, chalcocite, digenite, covellite, and pyromorphite. (Dolníček, Nepejchal and Vrtiška, 2024, pp. 8-9). Samples were taken from the eastern part of

the quarry, on the second to third benches of the northwest wall, from a disturbed geothermal vein approximately 50 cm thick, containing a large amount of copper minerals. Collected samples included malachite, azurite, and chrysocolla, with smaller amounts of chalcopyrite (See Figure 5). The copper minerals occurred predominantly as coatings, but also in more massive specimens.

The third copper ore consisted of very pure malachite samples from the Shilu site in China. This material served a comparative role as 'ideal' malachite of high purity, which is currently practically absent in the Czech Republic. For obvious reasons, these samples were not obtained through field prospecting but were purchased from a private collector. In this way, a relatively large amount of malachite from this site was secured with some pieces containing small amounts of so-called native copper. From a geological perspective, the Shilu site is a large polymetallic Fe-Cu-Co ore deposit located on Hainan Island in southern China (Chen, Zhou and Tang, 2022, p. 1415). The ore bodies are primarily located within the Shilu group, which consists of six units, traditionally numbered one to six from bottom to top. The Fe–Cu–Co ore bodies are mainly stratiform and are primarily hosted in Ca-silicate–rich dolomites and marbles, or in the metaclastic rocks of unit six (Chen, Zhou and Tang, 2022, pp. 1417–1419).

If we compare the samples with one another, it can be observed that the samples from the Shilu site in China exhibit very high purity already on the basis of visual inspection, containing almost no gangue. When some pieces were broken, native copper and cuprite were sometimes visible on the fracture surfaces. The size of the malachite ore fragments reached a few centimetres.

In the case of the Štěpánov nad Svratkou site, gangue was present to a greater extent. The character of the samples was not as qualitatively homogeneous as in the case of malachite from China, and the mineral composition was more variable. However, this was primarily due to the collection of samples from secondary deposits in front of the Mír shaft, where high-quality ore had undoubtedly already been extracted, and what was collected was essentially residual material. Despite these circumstances, the samples still contained a number of compact ore fragments of virtually pure malachite, again reaching sizes of a few centimetres. Among the samples, there were also many large rock fragments on which the copper ore occurred only as a surface coating.

In the case of the Lipová-lázně site, we can observe the highest overall proportion of gangue and, at the same time, the lowest degree of homogeneity. The character of the ore is strongly influenced by its hydrothermal origin. It consists of relatively thin layers of secondary copper minerals intermixed with gangue on large rock fragments of quartz. High-quality compact ore fragments were present only rarely and reached sizes of around one centimetre. In addition, non-compact dark green ore fragments occurred, intermixed with dark-coloured gangue.

Copper Content and Elemental Signature of the Ores

For the purpose of a preliminary determination of copper content in the ore samples, measurements were carried out using a benchtop XRF spectrometer ElvaX Pro equipped with an Ag X-ray tube, under the following conditions. The 'Soils' measurement mode was applied with dual task (light and heavy task), 5 mm collimator with helium purge for higher sensitivity of light elements). The light task was performed at a voltage of 8 kV and a current of 100 μA, without filters, with an acquisition time of 30 s. The heavy task was performed at a voltage of 35 kV and a current of 10 μA, using an 800 μm Al filter, with an acquisition time of 60 s. Three samples from each site were measured, and the results were subsequently averaged. Although this method is not suited for determining the content of light elements, it is acceptable with a certain degree of critical caution. Given that the aim of this analysis was essentially to establish only an approximate copper content, with accuracy to whole percentage points, the method is applicable. The results (See Table 1) show that ore samples from the Shilu site in China exhibit relatively high purity, with an average copper content of 53%, which is fairly close to that of pure malachite (57.5%). The overall quality of this ore is also reflected in the low content of elements representing gangue material. Calcium reaches 1%, while silicon reaches 3%. The second-highest, though noticeably lower, copper content was recorded in samples from the Štěpánov nad Svratkou site, which reached an average of 34%. In this case, the elements representing gangue material intergrown with the ore are present in higher concentrations. Calcium reaches 2%, while silicon is as high as 16%. The lowest copper content was observed in samples from the Lipová-lázně site (30%). Here, the presence of gangue-related elements is the highest. Silicon reaches 16%, as in the case of ores from the Štěpánov nad Svratkou site. However, calcium is present in a higher proportion, reaching 9%. Given the measurement accuracy, it is not appropriate to draw any further observations from these data.

Site	China	China	China	**China average**	Stěpánov nad Svratkou	Stěpánov nad Svratkou	Stěpánov nad Svratkou	**Stěpánov nad Svratkou average**	Lipová-lázně	Lipová-lázně	Lipová-lázně	**Lipová-lázně average**
Sample type	Ore	Ore	Ore		Ore	Ore	Ore		Ore	Ore	Ore	
Cu (%)	55	55	48	53	32	42	27	34	33	29	29	30
Cu +/- (%)	0,1	0,1	0,1	0,1	0,1	0,1	0,1	0,1	0,1	0,1	0,1	0,1
LE (%)	25	24	26	26	39	26	39	36	34	36	36	36
LE +/- (%)	0,2	0,2	0,1	0,17	0,1	0,2	0,1	0,13	0,1	0,1	0,1	0,1
Si (%)	4	2	4	3	16	11	21	16	13	18	17	16

Si +/- (%)	0,1	0,1	0,1	0,1	0,1	0,1	0,1	0,1	0,1	0,1	0,1	0,1
Ca (%)	0	2	0	1	3	2	2	2	9	9	8	9
Ca +/- (%)	0,1	0,1	0,1	0,1	0,1	0,1	0,1	0,1	0,1	0,1	0,1	0,1
Cl (%)	11	10	13	11	3	6	6	5	4	3	3	3
Cl +/- (%)	0,2	0,2	0,2	0,2	0,1	0,2	0,1	0,13	0,1	0,1	0,1	0,1
Mn (%)	0	0	0	0	0	0	0	0	2	1	2	1
Mn +/- (%)	0,1	0,1	0,1	0,1	0,1	0,1	0,1	0,1	0,1	0,1	0,1	0,1
P (%)	3	2	2	2	1	2	1	1	1	1	1	1
P +/- (%)	0,1	0,1	0,1	0,1	0,1	0,1	0,1	0,1	0,1	0,1	0,1	0,1
Ba (%)	1	4	3	3	4	3	3	3	1	1	1	1
Ba +/- (%)	0,3	0,2	0,2	0,23	0,2	0,2	0,2	0,2	0,2	0,2	0,1	0,17
Fe (%)	0	0	1	0	1	4	1	2	2	1	2	2
Fe +/- (%)	0,1	0,1	0,1	0,1	0,1	0,1	0,1	0,1	0,1	0,1	0,1	0,1
Ag (%)	0	0	0	0	0	1	0	0	0	0	0	0
Ag +/- (%)	0,1	0,1	0,1	0,1	0,1	0,1	0,1	0,1	0,1	0,1	0,1	0,1
K (%)	1	0	2	1	1	1	0	1	0	0	0	0
K +/- (%)	0,1	0,1	0,1	0,1	0,1	0,1	0,1	0,1	0,1	0,1	0,1	0,1
Mg (%)	0	1	1	0	0	1	0	0	0	0	0	0
Mg +/- (%)	0,3	0,3	0,2	0,27	0,1	0,2	0,2	0,17	0,2	0,1	0,1	0,13
Co (%)	0	0	0	0	0	0	0	0	1	1	1	1
Co +/- (%)	0,1	0,1	0,1	0,1	0,1	0,1	0,1	0,1	0,1	0,1	0,1	0,1
Sb (%)	0	0	0	0	0	1	0	0	0	0	0	0
Sb +/- (%)	0,1	0,1	0,1	0,1	0,1	0,1	0,1	0,1	0,1	0,1	0,1	0,1

TABLE 1: RESULTS OF THE ELEMENTAL ANALYSIS OF THE ORES. COMPILED BY: FILIP ŠEVČÍK

The samples were also subjected to an additional XRF analysis focusing on qualitative and quantitative analysis of metallic elements that may migrate from the copper ore into the metallic copper during smelting. To determine the basic elemental signature of the ores, XRF analysis was again performed using the same benchtop ElvaX Pro spectrometer equipped with an Ag X-ray tube with different conditions as follows: 'Cu' measurement mode, heavy task with accelerating voltage 45 kV, current 270 μA, 5 mm collimator, Ni 300 μm + Al 300 μm filter, and a measurement time of 300 seconds. These measurement conditions allow reliable detection and quantification of metallic elements. The results of ore samples were compared with the final products of smelting experiments to identify which elements are or are not transferred from copper ores into the metallic copper during the smelting process.

If we examine the results (See Table 2), we can characterise the basic elemental signature of the ores in terms of metallic elements (light elements below titanium are excluded).

Considering the copper content, the highest values are reached by the ore samples from China (See Figure 6 A), in which copper content reached up to 99% in two cases. Among the accompanying elements in the ore samples from China, iron can be observed, reaching up to 1.53% in one case, as well as manganese, and in one instance, also lead and zinc. Overall, however, these ores contain a relatively small amount of accompanying metallic elements.

The second-highest copper contents are observed in ores from the Štěpánov nad Svratkou site (See Figure 6 B), where the maximum value exceeds 96%. The copper content, however, is more variable. Accompanying elements include iron, reaching up to 8% in one case, arsenic, silver, antimony, lead, and zinc. Even from this overview, it is evident that the purity of this ore is lower than that of the ore samples from China.

The lowest copper contents are found in samples from the Lipová-lázně site (See Figure 6 C). These samples are again relatively variable, with the highest value of copper slightly exceeding 91%. With regard to accompanying elements, a notably higher manganese content is observed, reaching up to 7.5%. Iron is also relatively abundant, with values up to 5.71%, as well as cobalt with a maximum content of 1.84% and nickel, which also exceeds 1%. In addition to the elements mentioned above, the ore contains an elevated amount of arsenic.

Site	China	China	China	**China average**	Stěpánov nad Svratkou	Stěpánov nad Svratkou	Stěpánov nad Svratkou	**Stěpánov nad Svratkou average**	Lipová-lázně	Lipová-lázně	Lipová-lázně	**Lipová-lázně average**
Sample type	Ore	Ore	Ore		Ore	Ore	Ore		Ore	Ore	Ore	
Cu (%)	99,69	99,81	97,86	99,12	96,5	89,31	95,08	93,63	84,92	91,14	84,6	86,89
Cu +/- (%)	0,03	0,022	0,021	0,024	0,022	0,025	0,024	0,024	0,03	0,02	0,04	0,031
Fe (%)	0,13	0,07	1,53	0,58	2,69	8,04	3,22	4,65	5,71	3,38	4,81	4,63
Fe +/- (%)	0,03	0,02	0,019	0,023	0,019	0,03	0,021	0,023	0,03	0,03	0,04	0,033
Mn (%)	0,05	0,02	0,26	0,11	0,03	0,05	0,06	0,04	5,71	3,44	7,5	5,55
Mn +/- (%)	0,018	0,014	0,013	0,015	0,012	0,015	0,013	0,013	0,03	0,02	0,03	0,027
As (%)	0,02	0,02	0,02	0,02	0,29	0,39	0,22	0,3	0,35	0,2	0,26	0,27
As +/- (%)	0,005	0,003	0,005	0,004	0,006	0,01	0,007	0,008	0,006	0,005	0,006	0,006
Ag (%)	0	0	0	0	0	0,41	0,44	0,28	0	0	0	0
Ag +/- (%)	0,002	0,001	0,001	0,001	0,001	0,003	0,003	0,002	0,001	0,001	0,001	0,001
Sn (%)	0,03	0,03	0,03	0,03	0,02	0,04	0,03	0,03	0,03	0,03	0,03	0,03

Sn +/- (%)	0,003	0,002	0,002	0,002	0,002	0,003	0,002	0,002	0,002	0,002	0,002	0,002
Sb (%)	0,01	0	0	0	0,11	0,45	0,13	0,23	0,03	0,01	0,01	0,02
Sb +/- (%)	0,003	0,002	0,002	0,002	0,002	0,004	0,003	0,003	0,003	0,002	0,003	0,003
Pb (%)	0,02	0,01	0,15	0,06	0,18	0,48	0,29	0,32	0	0	0	0
Pb +/- (%)	0,009	0,007	0,007	0,008	0,015	0,021	0,015	0,017	0,018	0,013	0,017	0,016
Co (%)	0,01	0,01	0,02	0,01	0,02	0,05	0,03	0,03	1,84	1,04	1,64	1,51
Co +/- (%)	0,011	0,008	0,011	0,010	0,013	0,023	0,014	0,017	0,023	0,017	0,024	0,021
Ni (%)	0	0	0	0	0	0	0	0	1,4	0,74	1,13	1,09
Ni +/- (%)	0,01	0,008	0,007	0,008	0,007	0,009	0,007	0,008	0,018	0,013	0,019	0,017
Zn (%)	0,04	0,03	0,11	0,06	0,12	0,75	0,49	0,46	0	0	0,01	0
Zn +/- (%)	0,03	0,02	0,017	0,022	0,017	0,022	0,018	0,019	0,022	0,02	0,025	0,022
Au (%)	0	0	0,01	0	0,02	0,02	0,02	0,02	0,01	0,02	0,01	0,01
Au +/- (%)	0,009	0,007	0,006	0,007	0,006	0,009	0,007	0,007	0,006	0,006	0,007	0,006

TABLE 2: RESULTS OF METALLIC ELEMENTS ANALYSIS IN THE ORE SAMPLES. COMPILED BY: FILIP ŠEVČÍK

Principle of Copper Ore Smelting

To evaluate and understand the process of copper ore smelting, it is crucial to also understand its chemical principles. This knowledge was not accessible to prehistoric smelters, but it allows us nowadays to understand the processes that were originally developed based on experience and tradition. This enables us to introduce certain methodological shortcuts in the procedures and their evaluation compared to prehistoric smelters.

The first step in the smelting process of malachite is the thermal decomposition (calcination) of malachite ($Cu_2CO_3(OH)_2$) to copper(II) oxide, accompanied by the release of carbon dioxide and water vapor (1). This calcination begins at relatively low temperatures (200–300°C), depending on the particle size (Aoki, Yamamoto and Koga, 2021, p. 15109), with the maximum reaction rate occurring around 380°C (Brown, Mackenzie and Gainsford, 1984, pp. 24). This step also increases the porosity of the material and prepares the oxidic phase for subsequent reduction (Aoki, Yamamoto and Koga, 2021, p. 15110).

$$Cu_2CO_3(OH)_2 \rightarrow 2\ CuO + CO_2 + H_2O\ (1)$$

The energy required to reach high temperatures and drive the reduction reactions is supplied by the combustion of carbon present in charcoal or hardwood. The reactions of carbon form an integrated cycle: it is first oxidised by oxygen to carbon dioxide (2a), then, in excess carbon, carbon dioxide is reduced to carbon monoxide (2b), which in turn reduces copper(II) oxide to metallic copper (2c) (Goldstein and Mitchell, 2011, pp. 2806). These reactions simultaneously generate heat and enable efficient reduction of the ore.

$$C + O_2 \rightarrow CO_2 \text{ (2a)}$$

$$CO_2 + C \rightarrow 2\ CO \text{ (2b)}$$

$$CuO + CO \rightarrow Cu + CO_2 \text{ (2c)}$$

The resulting metallic copper melts upon reaching its melting point of 1085°C. Droplets of molten copper accumulate at the lowest point of the reduction vessel due to gravity and coalesce into a continuous melt due to surface tension.

At temperatures around 1200°C, the smelting process is accompanied by the formation of a significant byproduct – slag. Slag is an amorphous to partially crystalline silicate melt composed primarily of oxides of iron, aluminium, silicon, calcium, and magnesium (Schlesinger, *et al.*, 2011, pp. 73). Its composition reflects contributions from both the gangue of the ore and the ceramic material of the crucible and furnace.

Although the bulk of slag solidifies as a glassy matrix, it commonly contains well-developed crystalline phases formed during cooling. The most typical crystalline components belong to the olivine group, particularly fayalite (Fe_2SiO_4). In addition, spinel-group minerals are often present. Magnetite (Fe_3O_4) may crystallize under locally oxidizing or fluctuating redox conditions, whereas hercynite ($FeAl_2O_4$) reflects the interaction between iron oxide and alumina. Pyroxene phases, such as hedenbergite ($CaFeSi_2O_6$), may also develop in more chemically complex systems where sufficient CaO is available (Bourgarit, 2019, pp. 205). Besides silicate and oxide phases, copper-bearing inclusions are frequently observed within the slag matrix. These occur either as copper sulphides or as droplets of metallic copper. Their presence reflects incomplete separation of the metallic phase from the slag and thus provides valuable insight into the efficiency of the smelting process.

Experiment

The experiment aimed to answer one main research question and several sub-questions. The main research question was whether local copper ores from the Moravian region were of sufficient quality to be successfully reduced to pure copper. The other research sub-questions were whether this result could be achieved using technology roughly corresponding to the Eneolithic period (using elder blow pipes), the maximum yield of these ores, the transfer of the ore's elemental signature into the final product and the chemistry of smelting byproducts. To address these research questions, a series of experimental smelts was conducted.

In addition to testing the suitability of the collected ores for smelting, different methods of charging the ore into the furnace were also experimented with. The first method involved a standard modern graphite crucible. Another method used was to charge in a clay ball, which created a partially isolated environment that reduced contamination of the molten ore by material from the furnace. The final method involved charging a larger amount of material

directly into the furnace. Experiments were also conducted with different air supplies to the furnace, using both lever-operated bellows and blow pipes from elder branches.

Whether an experiment was considered successful or not was defined by a single criterion: an experiment was regarded as successful if the ore was successfully reduced to metallic copper. In practical terms, a successful experiment was therefore characterised by the production of a copper lump or prills at the end of the reduction process carried out using prehistoric technologies. This was our main and essentially only criterion. To compare the results of individual smelts more precisely, the degree of success was subsequently evaluated in relation to the maximum possible theoretical yield and compared between the individual smelts.

Preparations

Furnace Preparation

Before the smelting itself, it was necessary to prepare the missing equipment. In the first phase, we constructed a partially sunken, hemispherical furnace with an outer diameter of 40 cm. First, a pit was dug, shaped to correspond to the intended furnace but slightly larger. This resulting 'bowl' was then coated with a daub mixture containing chopped straw, without any added temper. The main material for the daub was clay from Červený kopec in Brno (clay deposits of the local defunct brickyard), where the experiment was conducted. The thickness of the daub layer reached approximately 5 cm (See Figure 7). Once the furnace was coated up to ground level and dried, an unfired clay tuyere was added at an angle of about 45°, directing air into the lower third of the furnace. Next, a daub rim about 5 cm high was applied above ground level. The furnace was then left to partially dry overnight. The following morning, cracks formed during drying were patched, and a small fire was lit inside the furnace for final drying (See Figure 8).

Air Supply Preparation

The lever-operated bellows (See Figure 9) were available from previous experiments with dimensions circa 70x40x20 cm and volume circa 20 l. However, it was necessary to prepare hollow blow pipes to test an alternative air supply method for the smelting. Blowpipes were used for small-scale metalworking, as evidenced by ethnological and archaeological sources (Davey and Hayes, 2024, Figure 6; Meanwell, *et al.*, 2020). Conical blowpipe tips were prepared from daub. The material for these wooden blowpipes was chosen to be naturally occurring in Central Europe during prehistory. For this purpose, elder (*Sambucus nigra*) was chosen. Macrobotanical remains of the elder are commonly found in the territory of the Czech Republic in the context of prehistoric sites. Elder typically occurred in forest clearings and open woodland environments (Kočár, *et al.*, 2022, p. 325). Although elder branches are not naturally hollow, their core contains a soft, 'spongy' material that can be removed. Young branches, containing the largest proportion of soft core, were used to make the blow pipes.

In theory, making these hollow blow pipes is a fairly simple process. The process only requires removing the soft core; the practical challenge lies in achieving this. Initially, we tried using smaller branches to push out the core, but this only compacted it further. Next, the ends of the small branches used for core extraction were beveled, allowing for more efficient removal through a rotary motion. This allowed somewhat easier removal of the core, but progress remained limited. In some cases, a solid partition inside the elder branches prevented further removal of the core. The final procedure involved heating copper rods in a fire and burning out the inner parts of the branches. As a non-regional alternative, we also tried to use bamboo sticks, which were much easier to hollow. After successfully removing the cores, the bottom ends of the blow pipes were coated with daub to create a fire-resistant nozzle and left to dry near the fire (See Figure 10).

Ore Preparation

The next step in preparation was ore crushing. A granite block was used as the base, and river pebbles as the pestle (See Figure 11). The goal was to achieve the finest possible ore fraction, which would then enter the reduction process (See Figure 12). Pieces of ore with a minimal amount of gangue were selected for crushing, and any remaining gangue was separated from the ore during crushing.

Temperature Monitoring

To monitor temperature development in the furnace during the experiments, type K thermocouples (Omega U8A) were used in combination with a four-channel data-logging thermometer (Omega HH147U), enabling continuous, real-time temperature recording. Due to the size and construction of the furnace, the location and size of the highest-temperature zone were relatively localized and depended on the charcoal and ore charges, but it was situated in front of the tuyere leading to the bellows. The temperature was not measured directly in the crucible or clay balls, but circa 10 cm from the bottom of the furnace. The thermocouple was not positioned directly at the spot of maximum temperature within the furnace so as not to obstruct the charges, but close to the tuyere end; however, it still allowed consistent monitoring of the overall temperature development during the experiments. Type K thermocouples represented a significant limitation in measuring the temperature in the furnace due to their maximum temperature threshold, which lies around 1300°C. For this reason, whenever the temperature rose significantly above 1200°C, the thermocouples had to be removed from the furnace to prevent damage.

Smelting

In the first phase of the experiment, prior to each smelt of local ores, a series of test smelts was conducted. In total, eight test smelts of malachite from the Shilu mine were carried out. These were intended to verify the stability of the prepared furnace and to test the feasibility of the chosen metallurgical procedure. During the first series of test smelts, different

methods of loading the ore into the furnace were also tested. Graphite crucibles, clay balls, and direct charge of the ore into the furnace were used. In the subsequent phases of the experiment, the smeltability of local copper ores from Moravia was tested, utilizing the insights gained from the previous test smelts. In all cases, charcoal made from oak and beech wood (ranging in size from 2 to 5 cm, predominantly closer to 5 cm) served as the fuel, and a lever-operated bellows was used to supply air. Operating at an average rate of 20–25 strokes per minute, with a capacity of 20 liters per stroke, the bellows delivered 400–500 liters of air per minute into the furnace. The only exception in which the lever-operated bellows was not used was an experiment involving blow pipes made of elder which was the final phase of our experimental smelts.

The First Phase of the Experiment – Test Smelts of High-quality Malachite from China

The test smelts of malachite from China served as a training ground for different metallurgical procedures, for verifying the correct construction of the furnace, and generally to ensure that we were technologically prepared for smelting local copper ores, which were of lower quality. This phase was essentially an initial step using an almost ideal ore, free of gangue, where the reduction process was expected to be relatively straightforward. Within this series of smelts, we also had the opportunity to experiment with different methods of charging the ore into the furnace. The initial test smelts were carried out in graphite crucibles, as this method is relatively easy to control, allows observation of the reaction, and enables intervention to adjust smelting parameters if problems arise.

A total of five crucible smelts of malachite from China were conducted (See Table 3).

Smelt No.	Site	Charge type	Time (m)	max. Temperature (°C)	Ore input (g)	Theoretical max. yield (g)	Actual yield (g)	Yield (%)
Smelt No. 1	China	Crucible	135	1200	188	99,64	85	85
Smelt No. 2	China	Crucible	67	1220	126	66,78	50	75
Smelt No. 3	China	Crucible	105	1300	192	101,76	85	84
Smelt No. 4	China	Crucible	53	1200	150	79,5	50	63
Smelt No. 5	China	Crucible	75	1200	100	53	0	0
Smelt No. 6	China	Clay balls	41	1200	61	32,33	31	96
Smelt No. 7	China	Clay balls	116	1200	144	76,32	37	48
Smelt No. 8	China	Open charge	57	1200	443	234,79	134	57
Smelt No. 9	Štěpánov nad	Clay balls	155	1202	120	40,8	0	0

	Svratkou							
Smelt No. 10	Štěpánov nad Svratkou	Crucible	37	1264	125	42,5	16	38
Smelt No. 11	Lipová-lázně	Clay balls	43	1200	32	9,6	1,8	19
Smelt No. 12	China	Crucible	67	1204	137	72,61	48	66

TABLE 3. RESULTS OF THE EXPERIMENTAL SMELTS. COMPILED BY: FILIP ŠEVČÍK

In the first step, the crucible was filled with crushed ore, and the remaining volume was topped up with coarsely crushed charcoal to promote a reducing atmosphere (See Figure 13). The standard procedure for each smelt involved placing a crucible filled with crushed ore, which was then covered with coarsely crushed charcoal, and positioning it at roughly half the depth of the already preheated and running furnace. The crucible had to be worked into this depth using downward pressure and rotational movements, which pushed the charcoal out from beneath the crucible and allowed it to settle into the cleared space. Once the crucible was properly placed in the furnace, it was completely covered with fresh charcoal. Smelting then began with air supplied by lever-operated bellows, and new fuel was added when needed.

In our experiments, temperatures of around 1200°C were commonly reached, sufficient for the reduction reaction, although in some cases (Smelt Three), we were able to achieve temperatures of up to approximately 1300°C (See Table 3). Smelt Three also provides a clear example of temperature development in the furnace, showing oscillations caused by the bellows operation and temporary drops when new fuel was added (See Graph 1).

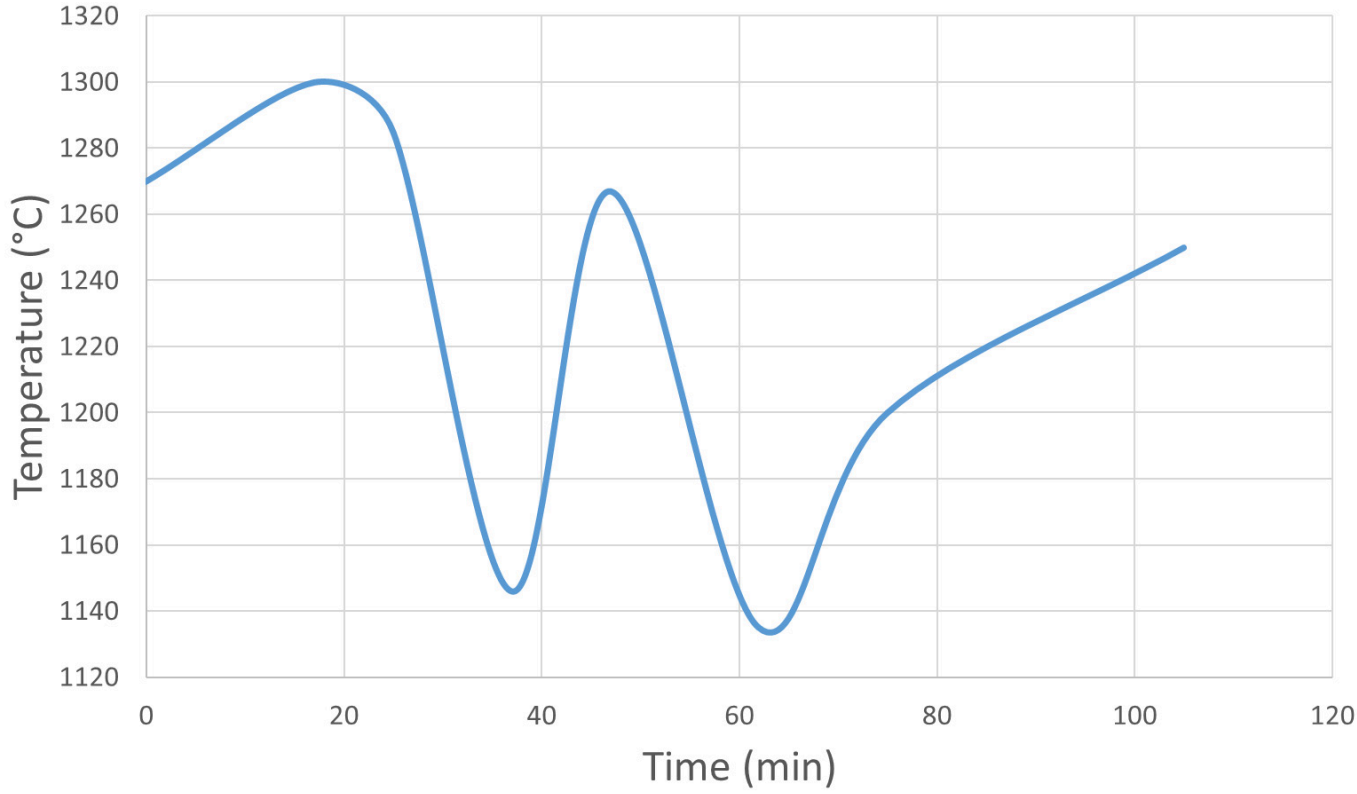

GRAPH 1. TEMPERATURE CURVE RECORDED DURING SMELTING THREE. CHART BY FILIP ŠEVČÍK

An important technological insight from the series of crucible test smelts was the necessity of allowing sufficient time for the ore to react. In almost all cases, the crucibles were removed after roughly 20 minutes to check their contents. At that point, the ore was generally undergoing some reduction reaction but was not yet fully reacted, and metallic copper had not yet formed (See Figure 14). Complete reaction in our test smelts typically occurred after approximately one hour in the furnace (See Table 3), represented by molten copper poured out of the crucible (See Figure 15).

In the next phase of test smelts of malachite from China, smelting in clay balls was tested. This method was explored primarily to obtain uncontaminated samples for later analyses, which is arguably its greatest advantage. On the other hand, unlike crucible smelting, it is not possible to observe the process and adjust parameters in case of an unfavourable course.

This procedure was tested in two smelts using a total of four clay balls. In all cases, the results were positive (See Table 3). Unlike crucible smelting, the process differed from the start, as the clay balls were prepared on-site during the first phase of the experiment. Local clay was used once again, with a small amount of hay added as temper. The clay was first shaped into a flat disc, and crushed ore mixed with lightly crushed charcoal was placed in the centre. The disc was then folded and formed into a ball, ensuring that the ore and charcoal mixture remained enclosed within a central pocket. The resulting balls had an average diameter of approximately 6 to 8 cm (See Figure 16). The balls were relatively wet and soft, so they had to be dried near the furnace before being placed inside. This drying took place during the

crucible smelts of the first test experimental phase. Once sufficiently dried, the clay balls could be inserted into the furnace.

Unlike graphite crucibles, the clay balls were relatively fragile and could not be pressed forcefully into the lower parts of the furnace. They were therefore only lightly pressed into the upper third of the furnace depth and covered with charcoal. During the smelting, as parts of the fuel burned away, the balls gradually sank toward the centre of the furnace. Temperatures in these test smelts again oscillated around 1200°C without major fluctuations, sufficient for the reduction reaction (See Table 3).

Since it was not possible to monitor the reaction directly, one pair of clay balls was removed after roughly 40 minutes (Smelt Six) and the second pair after about 90 minutes (Smelt Seven), with the intention of comparing the contents after cooling (See Table 3). After breaking all test balls, it was found that the reduction reaction had been fully completed in all four clay balls, with no macroscopically observable differences (See Figure 17).

A technological observation, reflecting the material used to make the clay balls, was the formation of a glassy slag layer on their surface. In later experiments, unrelated to this series of test smelts, some of the balls were fully melted, and the smelted copper subsequently flowed out into the furnace.

The final phase of the test smelts involved charging the ore directly into the furnace. This method makes it possible to obtain a relatively large amount of metal, since, unlike crucibles and clay balls, hundreds of grams of ore can be subjected to the reduction process at once. A clear disadvantage, however, is the need to allow the metal to cool down in order to retrieve it. The furnace needs to be emptied completely, and the smelting process needs to start all over again. For this reason, this charging method was tested only once, at the end of the series of test smelts.

For the purposes of this smelt, 234 g of ore was crushed and gradually added to the furnace in three stages (circa 75 g of ore each) of approximately ten minutes each. During this time, a temperature of around 1200 °C was maintained in the furnace by continuous operation of the lever-operated bellows (See Table 3). Each addition of ore was accompanied by a rather intense green flame (See Figure 18) radiating from the furnace, which in the past may have further reinforced the perceived symbolic significance of this metallurgical process.

After all the crushed ore had been added, the temperature was maintained for an additional 30 minutes (See Table 3). The bellows operation was then stopped, and the furnace was left to cool overnight. The following morning, the furnace was cleared of the remaining charcoal, and a big and still very hot copper lump containing embedded fragments of charcoal was recovered (See Figure 19 A), accompanied by a large number of smaller copper particles, most of which were also recovered from the furnace.

After the initial series of experiments with malachite from China, we observed quite interesting results. All test smelts were successful except for one (Smelt Five), resulting in a number of different copper lumps (See Figure 20) with an average yield relative to the theoretical maximum reaching 75% (See Table 3). These test smelts allowed us to verify the correct execution of the metallurgical procedures and construction of the furnace, enabling us to proceed with smelting less ideal ores from the Moravian region. From a technological perspective, several observations are noteworthy. Rather surprising was the good experience of smelting in clay balls. They were quite stable, very easy to handle. For example, there was no risk of losing material if they tipped over, and the reduction process proceeded relatively quickly due to the small ore charges and the enclosed construction, which retained heat well. Smelting in crucibles was somewhat more challenging in terms of handling, but this mainly concerned manipulating the crucible itself; the smelting process was not problematic. Compared to clay balls, crucibles likely experienced greater heat loss due to their open top, and combined with larger ore charges, the entire process took more time. While direct charging of ore into the furnace allows for the production of a larger total mass of metal in a single smelt, it proved to be less efficient in terms of the input-to-output ratio. In this case, we recorded one of the lower overall yields among the test smelts (57%, Table 3).

Second Phase of the Experiment – Smelting of Ore from the Štěpánov nad Svratkou Site

Based on the results of the test smelts, we decided to verify the smeltability of ore from the Štěpánov nad Svratkou site, first by smelting in clay balls and then by crucible smelting. In both cases, we followed a procedure similar to that used in the test smelts, including maintaining a temperature that again oscillated around 1200°C (See Table 3). Due to the limited amount of ore, we decided that in the case of the two clay balls, the temperature would be maintained for a longer period to allow the reaction to occur. However, even after more than two hours, no metallic copper was found when the balls were broken. For the second attempt, we chose crucible smelting so that the process could be observed. This attempt was considerably more successful, and after 37 minutes, molten copper was poured from the crucible, resulting in the creation of multiple copper lumps and spills (See Figure 20). The main goal of this part of the experiment was thus achieved, and the smeltability of this local ore was confirmed. The successful attempt reached a yield of 38% relative to the theoretical maximum.

Third Phase of the Experiment – Smelting of Ore from the Lipová-lázně Site

In the third phase of the experiment, we tested the smeltability of ore from the Lipová-lázně site. From a macroscopic perspective, this ore was the least suitable in terms of quality, although it exhibited an interesting signature of accompanying elements. Despite the very limited amount of material available, we decided, contrary to the results of the previous phase, to again use smelting in clay balls, as obtaining an uncontaminated metal sample was important for subsequent analyses.

For this phase of the experiment, two clay balls were prepared. Following the procedures verified in the previous experiments, they were placed into the preheated furnace, after a period of drying in radiating heat, and remained there for approximately 43 minutes while the temperature was maintained at around 1200°C (See Table 3). They were then removed from the furnace and, after cooling, broken open. The criterion for a successful smelt was fulfilled, as a large number of small droplets of metallic copper were found inside the balls (See Figure 21).

This granulation was caused by the overly fine fraction of charcoal that had been added to the clay balls to create a reducing atmosphere. While this fraction allowed the reaction to proceed, it prevented the individual droplets from forming a more compact copper lump. The yield relative to the theoretical maximum reached only 19% in this case, reflecting the relatively low quality of the ore.

Fourth Phase of the Experiment – Smelting Using Blow Pipes Made of Elder

In the final phase of the experiment, we aimed to verify whether a successful reduction of malachite to copper could be achieved using blowpipes made from elder. For this experiment, we used ore from China, which had proven relatively easy to reduce in the previous experiments, and we chose the crucible smelting method. The crucible was placed approximately halfway into the furnace, which had a temperature of around 1000°C at the time of insertion. Subsequently, six blowpipes were arranged in a circular pattern (See Figure 22) and air supply was initiated. About 30 minutes after the start of the process, the temperature reached approximately 1100°C. Although this is slightly above the melting point of copper, due to heat losses between the crucible and the furnace interior, the contents of the crucible had reacted but had not fully melted. Combined with the considerable physical effort required, particularly the fatigue experienced by the operators due to insufficient oxygen, and the gradual mechanical failure of the blowpipes, which began to burn and break near the clay tips, we decided to complete the smelt using a lever-operated bellows. With the bellows, we were able to raise the temperature to around 1200°C and complete the reaction. Even though our experiment using elder blowpipes was not successful in the end, it does not prove the unusability of wooden blowpipes in general. It just shows that bellows are a plausible alternative to the usually assumed use of blowpipes for Chalcolithic as shown in other experiments (Rose, Fabian and Goren, 2021).

Smelting Yield of Individual Ores

Out of a total of 12 smelts, ten were successful. If we evaluate only these ten successful smelts, it can be said that the efficiency of the smelts was relatively high. The overall yield reached 66%. The percentage yields are expressed relative to the theoretical maximum yield, which was calculated as the weight of the initial ore charge multiplied by the average copper concentration obtained from XRF measurements for the respective site, divided by 100. A

total of 1598 g of ore was used for all successful smelts, while theoretically 816 g of metal could have been obtained. The actual total yield reached 538 grams. The efficiency range was considerable: the highest yield, approaching the theoretical maximum, was 96% in Smelt Six. On the other hand, the lowest yield among the successful smelts was only 19% in Smelt 11.

The average yield varies significantly depending on the ore itself. The ore from China achieved the highest average yield of 68%. For these smelts, 1441 g of ore was used, with a theoretical maximum metal yield of 763 g, and the actual yield reached 520 g of copper. Next is ore from Štěpánov nad Svratkou, which achieved a yield of 38% in a single successful smelt, where 125 g of ore with a theoretical maximum of 42.5 g produced 16 g of copper. The lowest yield was recorded in the case of ore from Lipová-lázně, with 19% yield, where 32 g of ore with a theoretical maximum of 9.6 g yielded 1.8 g of copper.

These results closely reflect the overall quality of the ores from these sites, as discussed in the previous chapters.

Chemical Composition of the Smelted Copper Lumps

To determine the chemical signature of the smelted copper lumps, XRF analysis was performed with the same procedure as for copper ores before experiments. The analysis was done using a benchtop ElvaX Pro spectrometer with an Ag X-ray tube under the following conditions: 'Cu' measurement mode, accelerating voltage 45 kV, current 270 µA, 2 mm collimator, Ni 300 µm + Al 300 µm filter, and a measurement time of 300 seconds. Each sample was measured three times, and the results were averaged, giving a total acquisition time of 900 seconds per sample. The copper lumps were not measured from the surface; the top layer was abraded with a corundum cutting disc with a fabric bond to expose the metallic core, ensuring that the results were not contaminated by surface impurities.

All obtained copper lumps are characterised by very high copper purity, exceeding 99% in all cases (See Table 4 - PDF attachment).

The lumps produced from ore from the China samples achieved the highest purity. The average copper concentration was 99.94%, with a maximum of 99.98%. The concentrations of all accompanying elements were below 0.02% in most cases. Among the minor elements, manganese was observed with a maximum of 0.07%, and in one copper lump, arsenic reached a maximum of 0.03%. Overall, these copper lumps can be described as pure, with minimal amounts of accompanying elements.

The copper lump from the Lipová site also shows high purity, but its chemical signature is different. Copper content reached 99.76%. An elevated manganese content of 0.10% is evident, along with arsenic at 0.05%, nickel at 0.03%, and cobalt at 0.03%. Overall, this lump

can be characterised as very pure copper with an increased amount of manganese and trace amounts of arsenic, nickel, and cobalt.

The copper lump from the Štěpánov site had the lowest copper content at 99.49%. Its main accompanying element is silver, with a concentration of 0.41%, and arsenic is present at 0.06%. This lump can therefore be described as pure copper with a silver admixture and trace amounts of arsenic.

From the performed analysis, it is clear that the elemental signature of certain elements is partially transferred into the final copper lumps. While most of the main ore impurities, such as iron, manganese, zinc, and lead, were transferred into the copper lumps only in minimal amounts or were not transferred at all, a number of elements were carried over more significantly during the smelting process.

As has been demonstrated in previous studies, trace elements redistribute among the metallic phase, slag, and, where relevant, the gaseous phase, depending on their oxygen affinity and sulphur activity when sulphur is present in the system. Trace elements occur in several structurally distinct forms. Elements such as nickel and tin readily dissolve in the α-Cu solid solution, remaining relatively homogeneously distributed in the matrix. While arsenic, silver, and antimony occupy an intermediate structural position, they are still partially soluble in the α-Cu phase. In contrast, elements with very limited solubility, such as lead and bismuth, precipitate upon solidification as discrete metallic phases, typically segregated at grain boundaries. A distinct category comprises non-metallic inclusions formed by the conversion of certain elements into oxides and sulphides such as copper, arsenic and antimony (Scott and Schwab, 2019, pp. 89–96, 137).

In our case, we can mention that silver was transferred from the Štěpánov ore so effectively that it became the dominant characteristic impurity in the resulting copper lump. Elements such as cobalt and nickel were also transferred in smaller but measurable quantities. Despite the low overall transfer, in the case of the Lipová-lázně site, these elements transferred a unique ore signature into the copper lump.

To quantify trace element redistribution, absolute transfer rates were calculated (Transfer% = [mass of element in output / mass of element in input] × 100; Table 5). While the limited number of successful runs warrants caution, the resulting metrics highlight some contrast between final elemental concentrations and their actual transfer efficiencies. For instance, in the Štěpánov nad Svratkou, approximately 52% of the total input silver transferred into the metallic phase. On the other hand, the characteristic trace elements of the Lipová-lázně ores (Ni, Co, Mn) demonstrated extremely low transfer efficiencies, all falling below 0.6%. Their presence in the final copper is therefore primarily a result of their high initial concentrations in the source ore rather than a high transfer rate. This observation also clarifies the seemingly high cobalt transfer rates (24–47.5%) recorded in some China ore smelts. Since cobalt was

present in only trace amounts (0.01%) in the raw China ores, these elevated figures are likely due to the measuring limitations of XRF at such low concentrations. Additionally, the data reveal near-zero absolute transfer rates for iron (Fe) across all sites and methods. Despite its substantial presence in the raw ores, iron transfer consistently remained below 1%, demonstrating the high efficiency of the slagging process in separating iron from the metallic copper mix.

Furthermore, the data suggest that the smelting method itself significantly influences elemental partitioning, particularly for volatile elements. For the China ores, smelts conducted using clay balls generally exhibited higher average transfer rates for several trace elements compared to crucible smelts, where these elements were largely lost. For example, elements such as lead and zinc demonstrated noticeably enhanced retention within the enclosed clay ball systems. However, a closer examination of the individual clay ball experiments (Smelts 6 and 7) reveals significant internal variability. While lead and zinc showed enhanced retention across both experiments, the retention of elements such as arsenic and tin was highly inconsistent. Specifically, the notable average arsenic transfer (18.0%) was driven entirely by a single specific smelt (retaining 36%), whereas in the second clay ball smelt, the arsenic completely volatilised (0% transfer). Similarly, tin retention spiked to nearly 53% in one clay ball, but dropped below crucible averages (18.7%) in the other. This trend points to the possibility that the enclosed micro-environment within the clay ball restricts volatilization and alters local redox conditions, allowing elements that would otherwise escape into the atmosphere or pass into the slag to be better retained in the metallic phase. However, as the highly variable retention of specific volatile elements demonstrates, conditions within these micro-environments were likely fluctuating and difficult to control. The chemical profile of a copper lump can therefore be seen as a selective imprint of the chemical composition of the ores, created by the partial transfer of certain elements during smelting. This phenomenon can be observed in the case of the Štěpánov nad Svratkou ore, where silver content became the defining feature, and in the Lipová-lázně ore, where the defining signature is the combination of manganese, cobalt, and nickel.

Furthermore, the raw data suggest that the smelting method may significantly influence elemental partitioning and the overall consistency of the thermodynamic system. Crucible smelts for the China ores appeared to provide a relatively predictable environment. For instance, absolute tin (Sn) transfer in crucibles was notably stable, consistently clustering between 24% and 29%. Highly volatile elements such as zinc (Zn) were entirely lost to volatilisation, showing 0% transfer, while arsenic (As) was also lost in three out of four experiments, with the single exception of Smelt 12 which retained 10.9%. Lead (Pb) transfer in crucibles remained minimal, staying below 5% across all experiments.

The open charge method, represented by Smelt 8, displayed a seemingly distinct partitioning pattern. While its absolute tin transfer of 25.1% was comparable to the crucible baseline, and

both zinc and arsenic completely volatilized to 0% transfer, lead retention was noticeably higher, reaching 12.6%. This could imply that the open charge process, despite being an unenclosed system, might allow for different elemental interactions than the crucible method.

In contrast, smelts conducted within enclosed clay balls (Smelts 6 and 7) seem to have generated a micro-environment characterized by pronounced internal variability. Rather than a uniform enhancement of trace element retention, the clay balls exhibited a wider dispersion of transfer rates compared to the other methods. While this enclosed setup prevented the complete loss of highly volatile elements like zinc, retaining 1.3% and 15.8%, and lead, retaining 8.0% and 18.5%, the retention levels varied considerably between the two experimental runs. This variability is particularly evident in the behavior of tin and arsenic. In one clay ball (Smelt 6), tin retention increased to nearly 53% while arsenic completely volatilized to 0%. In the other (Smelt 7), tin retention decreased to 18.7% while arsenic transfer rose to 36.0%. These fluctuations point to the possibility that while the enclosed clay balls likely restrict the escape of volatile gases and alters local redox conditions, thereby potentially facilitating the retention of elements that would otherwise escape into the atmosphere or pass into the slag, the precise conditions within these micro-environments were presumably fluctuating and appear challenging to standardise during the process.

An interesting observation is the transfer of arsenic, particularly in comparison with Mondsee-type copper. From our experimental smelts, it is apparent that some transfer of arsenic from ore to copper occurs, but only to a limited extent. In the case of samples from China, where arsenic was scarcely present even in the ore itself (See Table 2), it was practically absent in the resulting copper (See Table 4 - PDF attachment). For the sites Lipová-lázně and Štěpánov nad Svratkou, where arsenic occurred in the ores at the level of tenths of a percent (See Table 2), it appears in the smelted copper at the level of hundredths of a percent (See Table 4 - PDF attachment). From this, we can suggest that in Mondsee-type copper, which may contain up to single-digit percentages of arsenic (Pernicka and Frank, 2015, p. 79), some deliberate addition of arsenic was likely involved, for example, by adding arsenic-bearing ore during smelting. To illustrate this quantitatively using our experimental data for the China ores: 100 g of this ore has a theoretical maximum yield of 53 g of copper. With an average practical recovery rate of 68% relative to this maximum, 100 g of ore produces approximately 36 g of actual metallic alloy. Achieving a 1% arsenic concentration in this final metal requires successfully retaining roughly 0.36 g of arsenic during the smelt. Under the optimal retention conditions observed in our enclosed clay ball experiments (retaining 36.0% of input arsenic), the raw 100 g ore charge would need to contain only 1.0 g of arsenic (a 1.0% initial concentration) to yield a 1% arsenical copper alloy. Conversely, under the poor retention conditions of an open crucible (using our lowest non-zero individual transfer of 10.9%), the starting ore would need to contain at least 3.3 g of arsenic (a 3.3% initial concentration) to achieve the identical final alloy. If average crucible losses are applied (2.7% transfer), the

required starting concentration surges to over 13%. This quantitative disparity suggests that the production of Mondsee-type arsenical copper likely depended not only on the deliberate addition of arsenic-rich ores, but also on utilizing smelting techniques that restricted volatilization.

Smelt No.	1	2	3	6	7	8	10	11	12
Site	China	China	China	China	China	China	Štěpánov nad Svratkou	Lipová-lázně	China
Charge type	Crucible	Crucible	Crucible	Clay balls	Clay balls	Open charge	Crucible	Clay balls	Crucible
As trans. (%)	0,0	0,0	0,0	0,0	36,0	0,0	7,4	3,2	10,9
Ag trans. (%)	-	-	-	-	-	-	52,0	-	-
Sn trans. (%)	28,2	24,7	27,6	52,8	18,7	25,1	11,7	5,4	29,1
Sb trans. (%)	-	-	-	-	-	-	1,5	0,0	-
Fe trans. (%)	0,0	0,0	0,0	0,0	0,7	0,0	0,0	0,0	0,0
Ni trans. (%)	-	-	-	-	-	-	-	0,5	-
Mn trans. (%)	2,6	2,2	2,5	10,1	24,8	12,0	2,9	0,3	9,9
Co trans. (%)	28,2	24,7	0,0	47,5	24,0	37,7	3,9	0,3	43,7
Pb trans. (%)	0,0	0,0	4,6	18,5	8,0	12,6	0,0	-	0,0
Zn trans. (%)	0,0	0,0	0,0	15,8	1,3	0,0	0,0	-	0,0
Au trans. (%)	-	-	-	-	-	-	0,0	0,0	-

TABLE 5: AVERAGE ABSOLUTE TRANSFER RATES OF TRACE ELEMENTS FROM ORE TO SMELTED COPPER. COMPILED BY: FILIP ŠEVČÍK

Chemical Composition of Smelting Byproducts

As established in the preceding chapters, the separation of metal from the gangue is never absolute. The investigation of slag polished cross-sections allows for a detailed assessment of the frequency and distribution of copper prills within the smelting byproducts. Given that direct temperature measurement via a thermocouple was not feasible within the crucible during the experiment, the mineralogical composition and phase assembly of the slag serve as a primary proxy for the thermal conditions.

The slag polished cross-sections were analysed by micro-XRF using an M6 Jetstream instrument equipped with a microfocus X-ray tube with an Rh anode. Data acquisition was performed using dual XFlash 6-60 silicon drift detectors under the following operating conditions: accelerating voltage 50 keV, current 600 µA, spot size 50 µm, step size 30 µm, and a dwell time of 30 ms per pixel. The microstructure is characterised by intergrown olivine-, spinel-, and pyroxene-rich phases (See Figure 23). Within this matrix, quartz inclusions and

variably sized metallic copper prills are clearly identifiable. These prills were entrapped within the slag matrix during solidification (See Figure 24). The presence of specific silicate phases, such as olivine and pyroxene, indicates that temperatures within the reaction zone reached at least 1200°C. However, the survival of relict quartz inclusions suggests that these thermal conditions were not sustained long enough, or were not sufficiently high, to achieve a fully molten glassy state or the complete dissolution of the silica grains. Furthermore, the presence of these dispersed copper prills confirms that while the reduction of malachite was successful, the metal was only partially separated from the slag. Their entrapment is likely a result of the high viscosity of the silicate melt, which prevented the individual droplets from coalescing into a single metallic ingot.

Similarly, clay ball one from smelting event two was also subjected to micro-XRF analysis. The acquisition was conducted using the M6 Jetstream under the following parameters: accelerating voltage 50 keV, current 600 µA, spot size 50 µm, step size 50 µm, and a dwell time of 30 ms per pixel, with the AMS 500 µm engaged. The resulting elemental map clearly reveals copper prills adhered to the ceramic matrix. The presence of these prills indicates exposure to temperatures sufficient not only for copper melting but also for the incipient melting of the ceramic body. This localized vitrification of the clay allowed the metallic phase to react with and partially infiltrate the ceramic fabric. The entrapment of these prills further illustrates how the softened ceramic surface acted as a physical barrier, hindering the complete coalescence and recovery of the copper (See Figure 25).

Summary

During our series of experimental smelts, we were able to complete all four planned phases with a certain degree of success. In the first phase of the experiment, we successfully tested both our skills and the technical capabilities of our metallurgical installation for the reduction of high-quality ore from the Shilu mine in China. Within this series of test smelts, we also had the opportunity to experiment with different methods of charging the ore into the furnace. The knowledge gained from these tests was subsequently applied in the following phases of the experiment, which consisted of attempts to reduce ores from local deposits in Moravia. In both cases, we were successful with the ores from Štěpánov nad Svratkou and Lipová-Lázně, we were successful, and the smeltability of these ores was verified. Finally, we also tested the feasibility of conducting the reduction process using blowpipes made from elder. From our perspective, this method proved relatively difficult in terms of maintaining the necessary temperature and the durability of the blowpipes. Furnace temperatures with their use ranged only between 1000°C and 1100°C. Although this is theoretically sufficient for copper reduction due to thermal losses between the furnace and the crucible, the initial reaction phase occurred, but the temperature inside the crucible did not reach the level necessary to melt copper. Furthermore, the elder blow pipes quickly failed mechanically in the intense radiant heat, with their ends burning and breaking off, even though clay nozzles were present. Given

the technological complexity of preparing blow pipes and the general difficulty of maintaining temperature, despite some experiments confirming the theoretical feasibility of this method (Hanning, Gauss and Goldenberg, 2010; Shimada and Merkel, 1991), their use appears rather inefficient based on our results. Although the production of lever-operated bellows is significantly more complex, their effectiveness is incomparable to that of blow pipes. As an alternative, a bag bellows, pot bellows, or drum bellows could be used, which are probably technologically the easiest to manufacture and theoretically more efficient than blow pipes.

Among the other important technological observations are those related to the different methods of charging the ore into the furnace. The crucible method proved to be relatively optimal in terms of allowing control over the reaction and enabling adjustments to the smelting conditions if necessary. Clay balls, on the other hand, did not allow such control, but they appeared to be relatively stable in maintaining temperature and in preserving the sample in an uncontaminated state. Charging the ore directly into the furnace excelled in enabling the reduction of larger quantities of ore, and an additional notable feature of this method was the pronounced coloration of the flame into shades of green. However, a certain disadvantage is the necessity to allow the furnace to cool down at least partially before the metal can be removed.

Micro-XRF analysis of slag cross-sections revealed olivine-, spinel-, and pyroxene-rich phases with quartz inclusions and entrapped copper prills, indicating temperatures of at least 1200°C. However, the presence of relict quartz suggests these conditions were not sustained long enough for complete melting and homogenisation of the slag.

The presence of copper prills within the slag matrix demonstrates that, although the reduction process was successful, metal separation remained incomplete. This is likely related to slag properties, particularly viscosity, which hindered copper droplets from coalescence into a single melt.

Another interesting observation is the imprint of the copper ore's chemical signature on the smelted copper lumps. The experimental results indicate that certain trace elements from the ore can be partially transferred into the resulting metal. This process appears to be selective, affecting only certain elements; however, in both cases where the ore exhibited a distinct chemical characteristic, this feature was also reflected in the final metal.

In the case of the Štěpánov nad Svratkou site, this involved an elevated presence of silver, whereas in the Lipová-lázně site it was the combination of manganese, cobalt, and nickel. This was most likely due to the occurrence of these metals in relatively easily reducible compounds. These findings are of interest, for example, from the perspective of archaeological artefact provenance studies. Although this provenance approach has recently been justifiably reconsidered and often abandoned, in theory, under conditions of a highly specific chemical signature and a high degree of deposit homogeneity, there remains some

potential for its application. Following from this, the transfer of arsenic from the ore to the copper bloom, as already noted above, is particularly interesting, although it is quite limited. Especially in the context of Mondsee-type copper, which occurred across extensive areas of Europe during the Eneolithic, the highly inconsistent transfer of arsenic observed in our experiments suggests that some form of deliberate addition of arsenic to the final mix might have been involved. This observation should serve as a starting point for further experimental research, which should focus on replicating the chemical composition of Mondsee-type copper through the co-smelting of copper and arsenic-bearing ores.

Acknowledgements

The authors would like to thank everyone who participated in the experimental smelts and helped make them possible, especially Marek Hendrych, Vladimíra Lepltová, Adam Procházka, Zuzana Kopáčová, Matěj Lelovič, and David Hons. The authors would also like to thank Omnya s.r.o., and in particular Pavel Kurka, for providing access to the Lipová-lázně quarry and the opportunity to collect ore samples.

This research was supported by Masaryk University under the grant “Archaeological field prospecting, excavation and documentation VI” (MUNI/A/1582/2025) and by institutional support from the Czech Academy of Sciences, Institute of Archaeology, Brno (RVO: 68081758).

Attachment(s)

Table 4. Results of the elemental composition analysis of the products obtained from the experimental smelts. (80.76 KB)

Keywords furnace, kiln or oven
copper

Country China
Czech Republic

Bibliography

Aoki, Y., Yamamoto, Y. and Koga, N., 2021. Thermal decomposition of spherically granulated malachite: physico-geometrical constraints and overall kinetics. *Physical Chemistry Chemical Physics* 23(28): pp. 15107-15118. //doi.org/10.1039/D1CP02519H

Bourgarit, D., 2019. Mineralogy of slags: A key approach for our understanding of ancient copper smelting processes, in: G. Artili and R. Oberti, eds. *The Contribution of Mineralogy to Cultural Heritage* . Mineralogical Society of Great Britain and Ireland, pp. 203–232. https://doi.org/10.1180/EMU-notes.20.5

Brown, I.W.M., Mackenzie, K.J.D. and Gainsford, G.J., 1984. Thermal decomposition of the basic copper carbonates malachite and azurite. *Thermochimica Acta* 75, 23–32. https://doi.org/10.1016/0040-6031(84)85003-0

Burkart, E., 1953. *Moravské nerosty a jejich literatura* . Nakladatelství Československé akademie věd, Praha.

Chen, W.T., Zhou, M.-F., Tang, Y., 2022. New insights about the origin of the Shilu Fe-Cu-Co deposit, Hainan Island, South China, with emphasis on the regional metallogeny. *Mineralium Deposita* 57, 1415–1430. https://doi.org/10.1007/s00126-022-01113-3

Chmelíková, D., 2014. Ložiska měděné rudy u Mutěnína (okr. DO) v západních Čechách a otázka jejich využití v pravěku. *Acta Rerum Nat* . pp.19–32.

Davey, C.J. and Hayes, P.C., 2024. Out of the Fiery Crucible: Egyptian Old Kingdom metallurgy. *Buried History* , Aust. Inst. Archaeol. 59, pp.11–28. https://doi.org/10.62614/wmj1b145

Dolníček, Z., Nepejchal, M. and Vrtiška, L., 2024. Gersdorffit, tyrolit a Bi-minerály z žilné Cu mineralizace z lomu Smrčník u Lipové-lázní u Jeseníku (Česká republika). *Bulletin Mineralogie Petrologie* 32, pp.8–18. https://doi.org/10.46861/bmp.32.008

Goldstein, E.A. and Mitchell, R.E., 2011. Chemical kinetics of copper oxide reduction with carbon monoxide. *Proceedings of the Combustion Institute* 33, pp.2803–2810. https://doi.org/10.1016/j.proci.2010.06.080

Hanning, E., Gauss, R. and Goldenberg, G., 2010. Metal for Zambujal: experimentally reconstructing a 5000-year-old technology. *Trabajos de Prehistoria* 67. https://doi.org/10.3989/tp.2010.10040

Houzar, S., Hrazdil, V., Malý, K., Pfeiferová, A. and Sadílek, J., 2000. Charakteristika pozůstatků po starém dolování Ag-Pb-Cu rud ve štěpánovském rudním revíru na západní Moravě, in: *Západní Morava: vlastivědný sborník* . Brno, pp. 116–137.

Hunt Ortiz, M.A., 2003. *Prehistoric mining and metallurgy in South West Iberian Peninsula* . British Archaeological Reports, Oxford.

Kmošek, J., Augustýnová, M., Fikrle, M. and Erban Kochergina, Y.V., 2025. Bronze age casting cakes from the Domažlice region compared with the Mutěnín copper ore deposit in Western Bohemia (Central Europe). *Archaeological and Anthropological Sciences* 17, 229. https://doi.org/10.1007/s12520-025-02355-8

Kočár, P., Kočárová, R., Lanta, M. and Novák, J., 2022. Rekonstrukce lesní vegetace České republiky v zemědělském pravěku a raném středověku na základě archeoantrakologických dat

/ Reconstruction of Forest Vegetation Between the Neolithic and the Early Middle Ages in the Territory of the Czech Republic Based on Archaeoanthracological Data. *Památky Archeologické* 113, pp.311–368. https://doi.org/10.35686/PA2022.6

Kruťa, T., 1966 . *Moravské nerosty a jejich literatura 1940-1965* . Moravské muzeum, Brno.

Kruťa, T., 1973. *Slezské nerosty a jejich literatura* . Moravské muzeum, Brno.

Meanwell, J.L., Paris, E.H., Peraza Lope, C., Seymour, L.M. and Masic, A., 2020. Blowpipes and their metalworking applications: New evidence from Mayapán, Yucatán, Mexico. *PLOS One* 15, e0238885. https://doi.org/10.1371/journal.pone.0238885

Niederschlag, E., Pernicka, E., Seifert, Th. and Bartelheim, M., 2003. The Determination of Lead Isotope Ratios by Multiple Collector Icp-Ms: A Case Study of Early Bronze Age Artefacts and their Possible Relation With Ore Deposits of the Erzgebirge*. *Archaeometry* 45, 61–100. https://doi.org/10.1111/1475-4754.00097

O'Brien, W., 2014. *Prehistoric Copper Mining in Europe: 5500-500 BC* . Oxford University Press. https://doi.org/10.1093/oso/9780199605651.001.0001

Pařízek, J., 2000. *Dobývání nerostných surovin v okrese Žďár nad Sázavou a okolí, Listy Horáckého muzea* . Horácké muzeum, Žďár nad Sázavou.

Pernicka, E. and Frank, C., 2015. Das Kupfer der Mondseegruppe, in: T. Stöllner, and P. Thomas, eds. *Bergauf bergab: eine Zeitreise durch 10.000 Jahre Bergbau in den Ostalpen - Begleitbuch* zur Ausstellung Bergauf Bergab - 10.000 Jahre Bergbau in den Ostalpen im Deutschen Bergbau-Museum Bochum vom 31.10.2015 - 24.04.2016, im Vorarlberg Museum Bregenz vom 11.06.2016 - 26.10.2016, Veröffentlichungen aus dem Deutschen Bergbau-Museum Bochum. VML Verlag Marie Leidorf, Rahden/Westf.

Pernicka, E., Lutz, J. and Stöllner, T., 2016. Bronze Age Copper Produced at Mitterberg, Austria, and its Distribution. *Archaeologia Austriaca* 1, pp.19–56. https://doi.org/10.1553/archaeologia100s19

Radivojević, M., Roberts, B., Marić, M., Kuzmanović-Cvetković, J. and Rehren, T., eds., 2021. *The Rise of Metallurgy in Eurasia: Evolution, Organisation and Consumption of Early Metal in the Balkans.* Archaeopress Archaeology. https://doi.org/10.32028/9781803270425

Radivojević, M. and Roberts, B.W., 2021. Balkan metallurgy and society, 6200–3700 BC, in: M. Radivojević, B.W. Roberts, M. Marić, J. Kuzmanović-Cvetković and T. Rehren, eds. *The Rise of Metallurgy in Eurasia: Evolution, Organisation and Consumption of Early Metal in the Balkans* . Archaeopress Publishing Ltd, Oxford, pp. 11–37.

Rose, T., Fabian, P. and Goren, Y., 2021. Shedding New Light on the Pure Copper Metallurgy of the Chalcolithic Southern Levant Through an Archaeological Experiment. *EXARC Journal* 2021/4, https://exarc.net/ark:/88735/10601

Schlesinger, M.E., King, M.J., Sole, K.C. and Davenport, W.G., 2011. Matte Smelting Fundamentals, in: *Extractive Metallurgy of Copper* . Elsevier, pp. 73–88. https://doi.org/10.1016/B978-0-08-096789-9.10005-8

Scott, D.A. and Schwab, R., 2019. *Metallography in Archaeology and Art* . Springer Nature.

Shimada, I. and Merkel, J.F., 1991. Copper-Alloy Metallurgy in Ancient Peru. *Scientific American* 265, pp.80–87. https://www.jstor.org/stable/24936982

Točík, A. and Žebrák, P., 1989. Ausgrabungen in Špania Dolina – Piesky. Zum Problem des urzeitlichen Kupfererzbergbaus in der Slowakei, in: *Archäometalurgie Der Alten Welt. Der Anschnit* t. Beiheft 7. Bochum. pp. 71–78.

Zachar, T. and Salaš, M., 2019. Příspěvek k problematice distribuce středoslovenské mědi na Moravě v mladší době bronzové na příkladě kovových depotů Blučina 1 a Blučina 13. *Archeologické Rozhledy* 71, 615–640. https://doi.org/10.35686/AR.2019.25

Corresponding Author

Filip Ševčík
Department of Archaeology and Museology
Arna Nováka 1/1
602 00 Brno
Czech Republic
E-mail Contact

Gallery Image

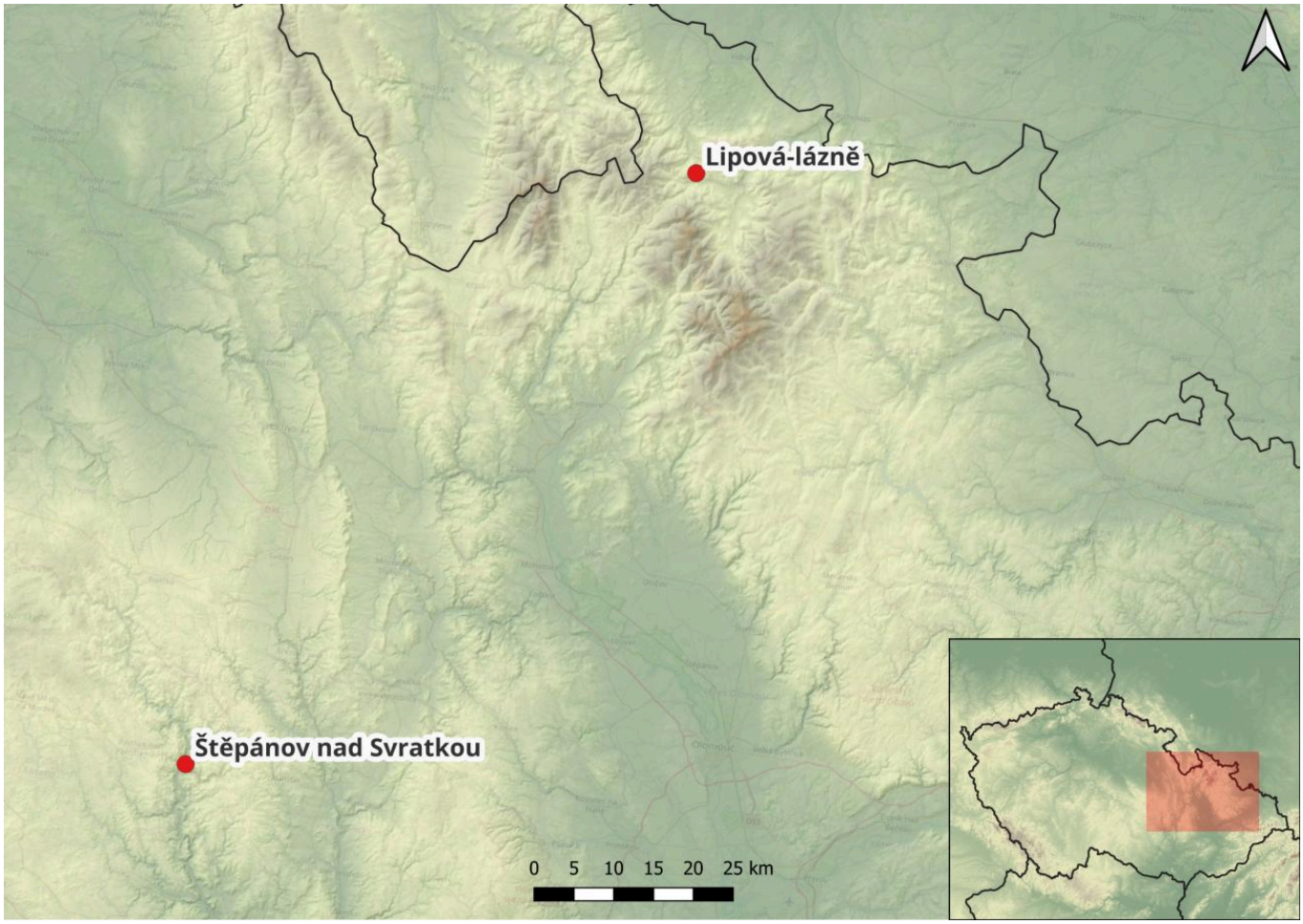

FIG 1. LOCATIONS OF THE ORE SAMPLING SITES IN MORAVIA. BASE MAP: OPENSTREETMAP. DEM: CZECH OFFICE FOR SURVEYING, MAPPING AND CADASTRE.

FIG 2. ORE COLLECTED DURING SURVEY AT THE ŠTĚPÁNOV NAD SVRATKOU SITE. PHOTO BY FILIP ŠEVČÍK

FIG 3. FRACTURE SURFACE OF AN ORE SAMPLE FROM THE ŠTĚPÁNOV NAD SVRATKOU SITE. PHOTO BY FILIP ŠEVČÍK

FIG 4. QUARTZ VEIN CONTAINING COPPER MINERALS AT THE LIPOVÁ-LÁZNĚ SITE. PHOTO BY FILIP ŠEVČÍK

FIG 5. FRACTURE SURFACE OF AN ORE SAMPLE FROM THE LIPOVÁ-LÁZNĚ SITE. PHOTO BY FILIP ŠEVČÍK

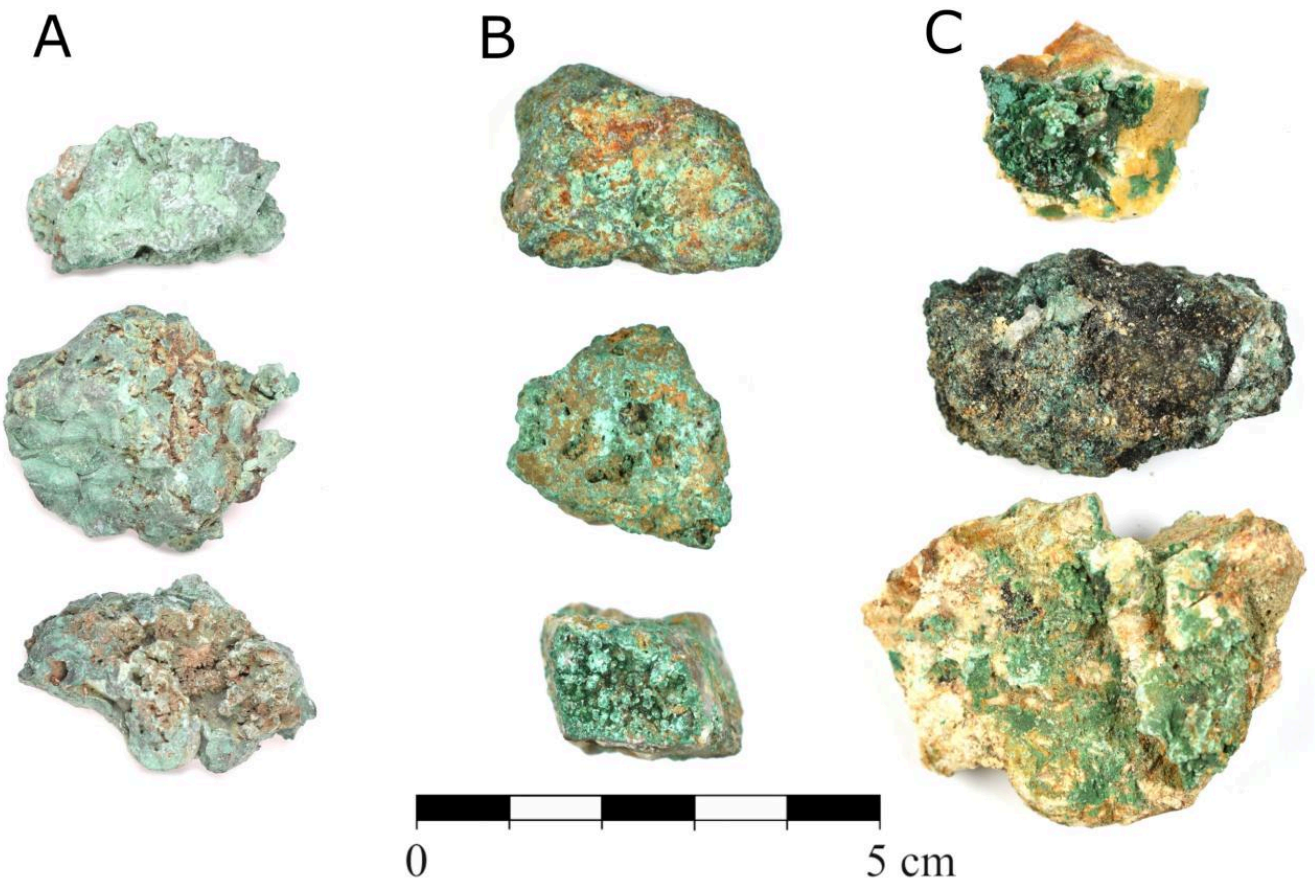

FIG 6. COPPER ORE SAMPLES: A – SHILU MINE, CHINA; B – ŠTĚPÁNOV NAD SVRATKOU; C – LIPOVÁ-LÁZNĚ. PHOTO BY FILIP ŠEVČÍK

FIG 7. FURNACE BEFORE DRYING. PHOTO BY FILIP ŠEVČÍK

FIG 8. FURNACE AFTER DRYING AND PREHEATING WITH CHARCOAL. PHOTO BY DAMIAN JIROUT

FIG 9. LEVER-OPERATED BELLOWS USED IN THE EXPERIMENT. PHOTO BY MATĚJ KMOŠEK

FIG 10. BLOWPIPES MADE FROM ELDER WOOD. PHOTO BY VLADIMÍRA LEPLTOVÁ

FIG 11. CRUSHING OF COPPER ORE. PHOTO BY DAMIAN JIROUT

FIG 12. CRUSHED COPPER ORE PREPARED FOR SMELTING. PHOTO BY FILIP ŠEVČÍK

FIG 13. FILLING OF THE CRUCIBLE WITH ORE AND CHARCOAL. PHOTO BY VLADIMÍRA LEPLTOVÁ (1) AND ADAM PROCHÁZKA (2)

FIG 14. PARTIALLY REACTED CHARGE INSIDE THE CRUCIBLE. PHOTO BY FILIP ŠEVČÍK

FIG 15. POURING MOLTEN COPPER FROM THE CRUCIBLE. PHOTO BY FILIP ŠEVČÍK

FIG 16. PREPARATION OF A CLAY BALL. PHOTO BY VLADIMÍRA LEPLTOVÁ

FIG 17. CLAY BALL AFTER BEING BROKEN OPEN FOLLOWING SMELTING. PHOTO BY FILIP ŠEVČÍK

FIG 18. GREEN FLAME PRODUCED DURING DIRECT CHARGING OF ORE INTO THE FURNACE. PHOTO BY FILIP ŠEVČÍK

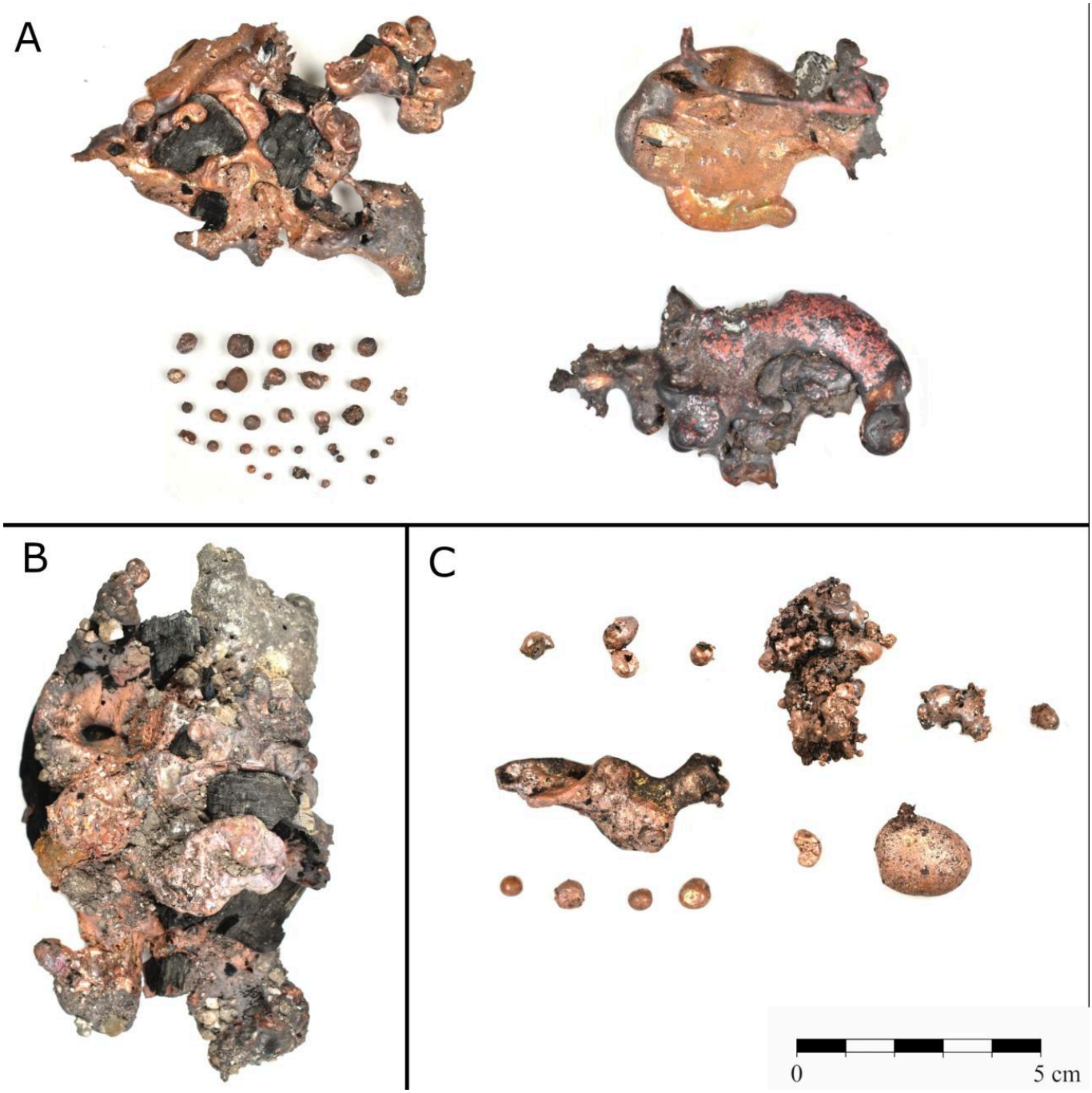

FIG 19. SELECTION OF COPPER LUMPS FROM THE FIRST PHASE OF EXPERIMENTAL SMELTS: A – CRUCIBLE SMELTS; B – DIRECT FURNACE CHARGE; C – SMELTS IN CLAY BALLS. PHOTO BY FILIP ŠEVČÍK

FIG 20. COPPER LUMPS PRODUCED FROM ORE SMELTED FROM THE ŠTĚPÁNOV NAD SVRATKOU SITE. PHOTO BY FILIP ŠEVČÍK

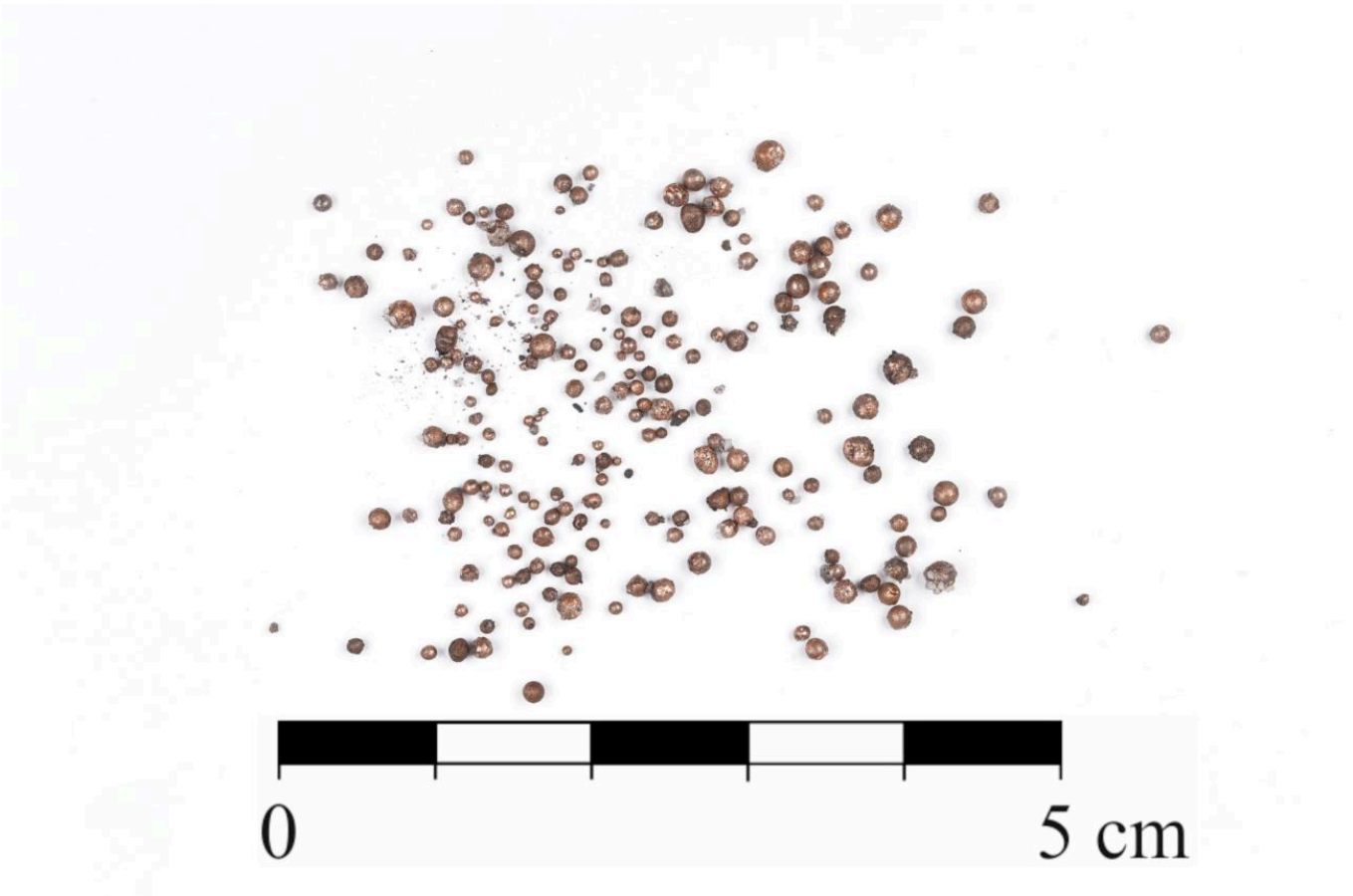

FIG 21. COPPER LUMPS PRODUCED FROM ORE SMELTED FROM THE LIPOVÁ-LÁZNĚ SITE. PHOTO BY FILIP ŠEVČÍK

FIG 22. USE OF ELDER-WOOD BLOWPIPES DURING SMELTING. PHOTO BY MATĚJ LELOVIČ

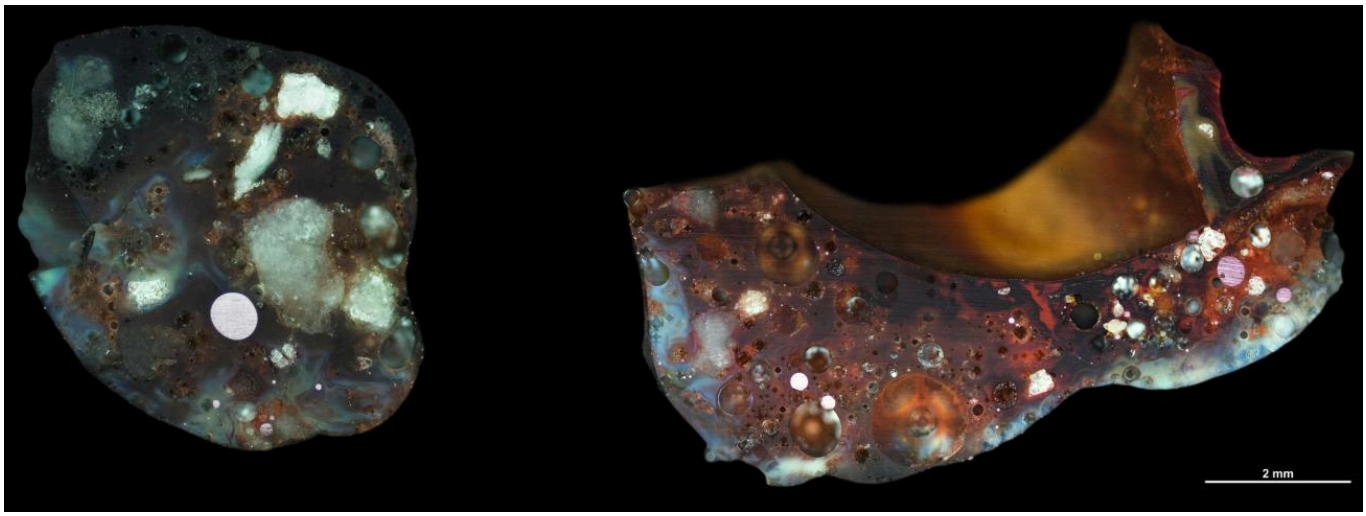

FIG 23. POLISHED SECTIONS OF SLAG DOCUMENTED UNDER AN OPTICAL MICROSCOPE. PHOTO BY ČENĚK FOUČEK

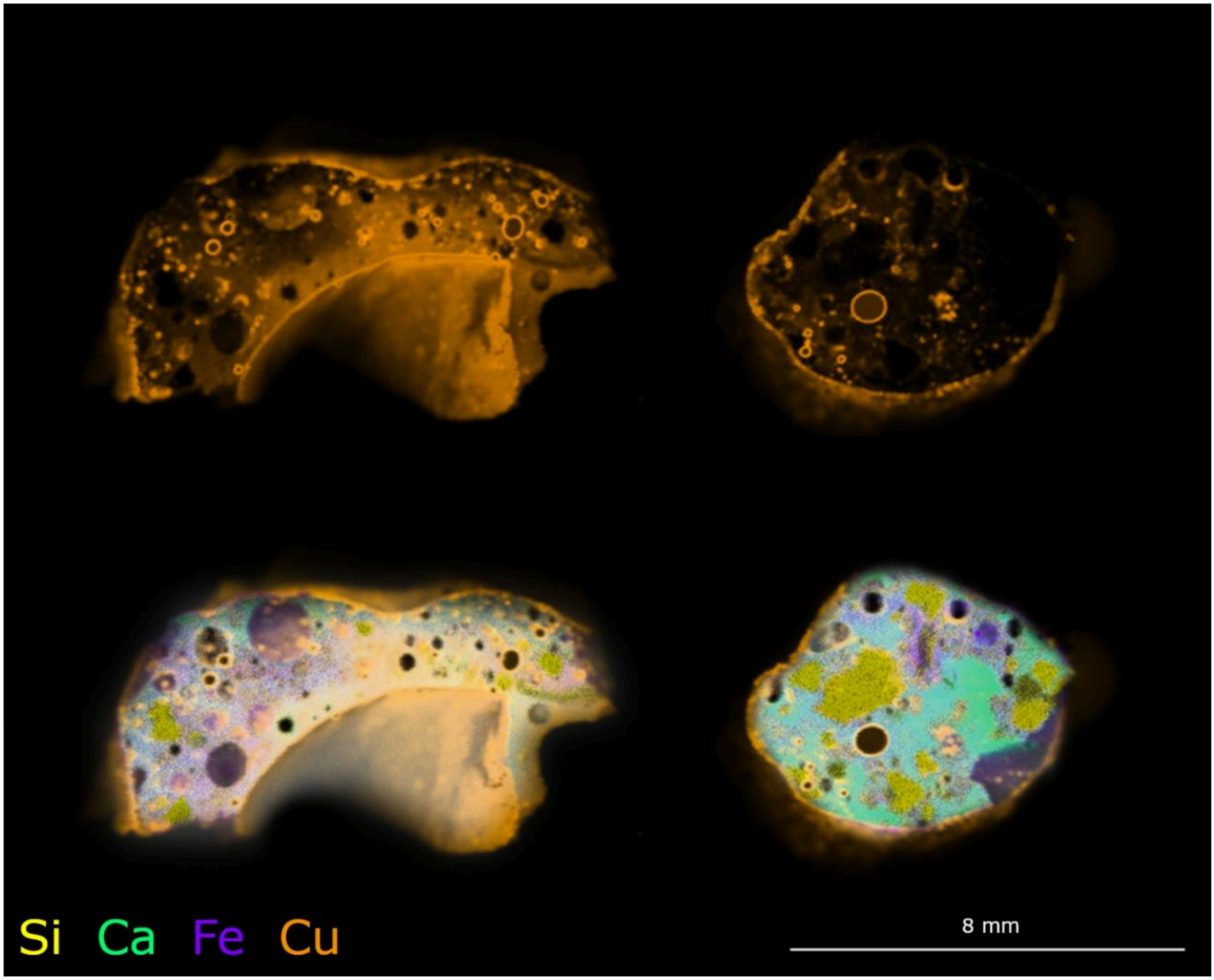

FIG 24. ELEMENTAL MAPS SHOWING THE MAIN COMPONENTS OF THE POLISHED SLAG SECTIONS OBTAINED BY MICRO-XRF. PHOTO BY ČENĚK FOUČEK

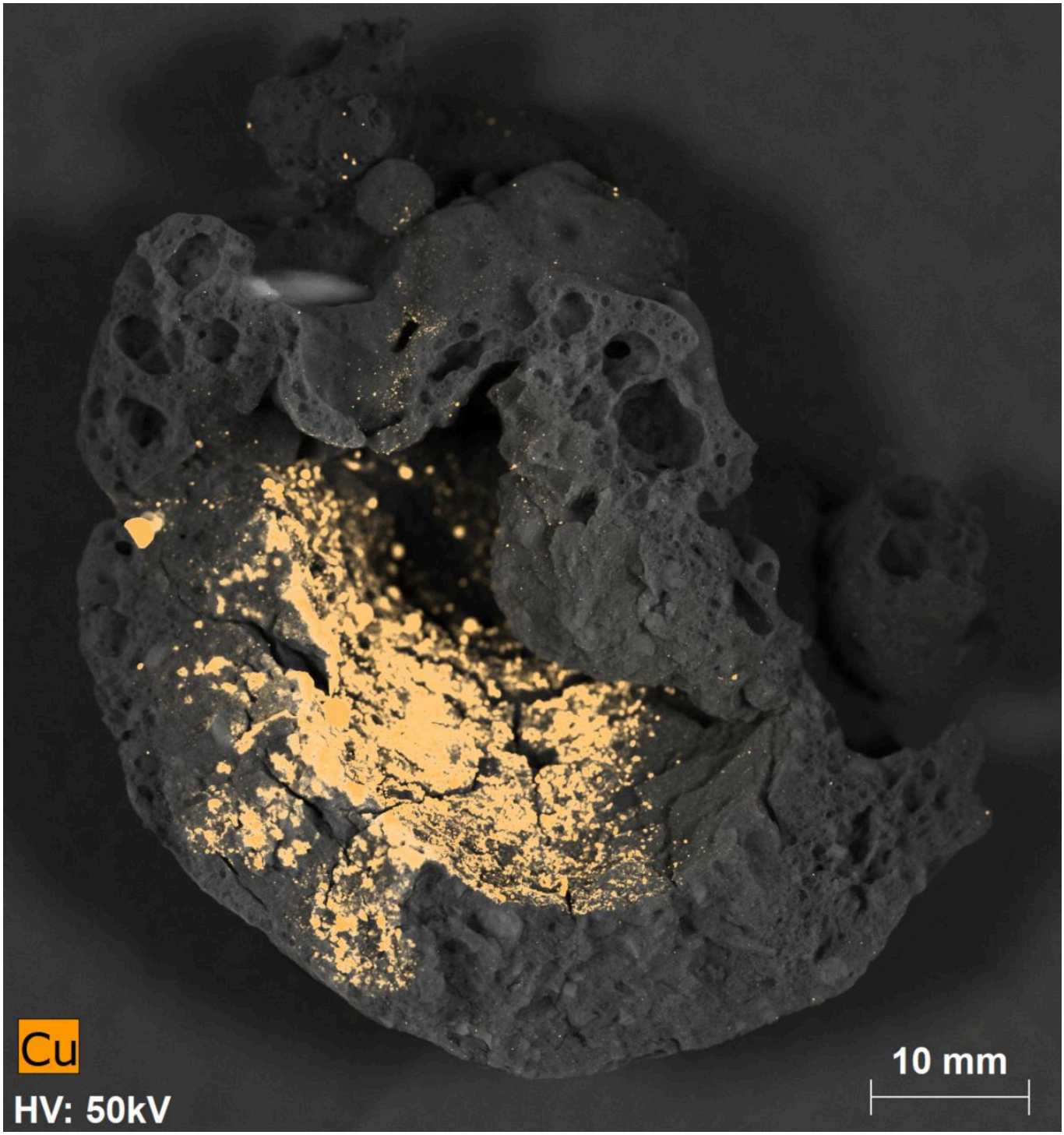

FIG 25. SPATIAL DISTRIBUTION OF COPPER WITHIN A CLAY BALL AFTER SMELTING OBTAINED BY MICRO-XRF. PHOTO BY ČENĚK FOUČEK